

Global trends and patterns of drought from space

Lisa Damberg · Amir AghaKouchak

Received: 20 June 2013 / Accepted: 16 September 2013 / Published online: 29 September 2013
© Springer-Verlag Wien 2013

Abstract This paper analyzes changes in areas under droughts over the past three decades and alters our understanding of how amplitude and frequency of droughts differ in the Southern Hemisphere (SH) and Northern Hemisphere (NH). Unlike most previous global-scale studies that have been based on climate models, this study is based on satellite gauge-adjusted precipitation observations. Here, we show that droughts in terms of both amplitude and frequency are more variable over land in the SH than in the NH. The results reveal no significant trend in the areas under drought over land in the past three decades. However, after investigating land in the NH and the SH separately, the results exhibit a significant positive trend in the area under drought over land in the SH, while no significant trend is observed over land in the NH. We investigate the spatial patterns of the wetness and dryness over the past three decades, and we show that several regions, such as the southwestern United States, Texas, parts of the Amazon, the Horn of Africa, northern India, and parts of the Mediterranean region, exhibit a significant drying trend. The global trend maps indicate that central Africa, parts of southwest Asia (e.g., Thailand, Taiwan), Central America, northern Australia, and parts of eastern Europe show a wetting trend during the same time span. The results of this satellite-based study disagree with several model-based studies which indicate that droughts have been increasing over land. On the other hand, our findings concur with some of the observation-based studies.

1 Introduction

Numerous studies indicate that the frequency of extreme events such as droughts has increased, particularly in the twentieth century (Trenberth 2001; Alexander et al. 2006; Dai 2012; Hao and AghaKouchak 2013b; Frich et al. 2002). Major drought events have been reported in the USA, the Horn of Africa, Australia, and southern Europe over the past few decades. Texas, for example, experienced two record droughts in 2011 and 2006, resulting in billions of dollars in economic losses (AghaKouchak et al. 2012a). Numerous model-based studies indicate that droughts and dry spells have increased in the second half of the twentieth century (e.g., Dai 2012).

Drought development is a slow and complex process that can be described using multiple indicators and variables. Droughts are often classified into four different categories: meteorological drought (deficit in precipitation), agricultural drought (deficit in soil moisture), hydrological drought (deficit in surface water, groundwater, reservoir storage), and socioeconomic drought (imbalance in water supply and demand)—see Wilhite and Glantz (1985). This study investigates global trends and patterns of meteorological droughts and drying areas using a satellite-based, model-independent data record. Hereafter, drought refers to a deficit in precipitation (Hayes et al. 1999).

The Standardized Precipitation Index (SPI; McKee et al. 1993), which is one of the most commonly used and recommended drought indicators, is used to describe meteorological droughts (WMO 2009; WCRP 2010). Negative and positive values of SPI indicate dry and wet periods, respectively. SPI values between -1 (≈ 20 th percentile) and -2 (≈ 5 th percentile) refer to moderate to severe droughts, while SPI below -2 indicates extreme droughts (McKee et al. 1993). Given the flexibility and simplicity of SPI, it has

L. Damberg · A. AghaKouchak (✉)
University of California Irvine,
E4130 Engineering Gateway Irvine,
Irvine, CA 92697-2175, USA
e-mail: amir.a@uci.edu

been widely used in drought studies (e.g., Mo 2008; Wang et al. 2011, 2013a; Shukla and Wood 2008).

Documenting changes in droughts requires long-term records of observations with suitable temporal and spatial coverage. Most studies of historical droughts have been based on analyses of long-term gauge (point) measurements of precipitation (e.g., Serinaldi et al. 2009; Shiau 2006). However, the spatial distribution of rain gauges is insufficient for providing reliable and homogeneous estimates of the spatial distribution of precipitation and, hence, droughts on a global scale (Easterling 2012). As is well known, the spatial extent is fundamental for understanding the drought phenomena (Andreadis et al. 2005). In addition to rain gauges, hydrological and climate model simulations have also been used to assess changes in drought occurrences and intensities (Robock et al. 2004; Sheffield et al. 2004; Anderson et al. 2011; Wehner 2012; Dirmeyer et al. 2006). Climate/hydrological models provide valuable gridded information on droughts. However, numerous studies have shown discrepancies in regional and global climate model simulations of precipitation patterns and, thus, drought spatial extent (WCRP 2010; Kirono and Kent 2011; Coelho and Goddard 2009).

Recent advances in developing global satellite precipitation data sets (e.g., Adler et al. 2003; Sorooshian et al. 2011) provide the opportunity to assess changes in the spatial extent of droughts over the past three decades. The advantages of using satellite precipitation data for drought monitoring include (a) consistent and homogeneous data in a quasi-global scale and (b) coverage over areas with no other means of observations (e.g., rain gauges and weather radars). The importance of using the emerging satellite data sets for drought monitoring, especially for validation and verification of model simulations, has been emphasized in previous studies (e.g., Wardlow et al. 2012). This paper documents changes in trends and patterns of meteorological droughts using satellite precipitation observations. The paper is organized as follows: after this introduction, the data set used in the study is discussed. The methodology and results are presented in Section 3, and the conclusions and final remarks are summarized in Section 4.

2 Data

We use a recently developed, merged monthly data set that combines the long-term Global Precipitation Climatology Project (GPCP; Adler et al. 2003) satellite data with near real-time satellite observations (TMPA-RT; Huffman et al. 2007 and PERSIANN; Sorooshian et al. 2000; Hsu et al. 1997) developed for drought analysis (AghaKouchak and Nakhjiri 2012). In the merged data set, the climatology is driven by the GPCP data, and the near past data

are based on near real-time satellite precipitation observations. The merging algorithm includes a Bayesian correction algorithm to ensure consistency of the two data sets for drought analysis and to reduce biases and uncertainties associated with satellite data discussed in previous studies (e.g., Turk et al. 2008; AghaKouchak et al. 2012b; Tian et al. 2009; Mehran and AghaKouchak 2013). The algorithm and the overall quality of the data set are tested and validated for the period of overlap (2000–2010) between GPCP and both TMPA-RT and PERSIANN (see AghaKouchak and Nakhjiri 2012). The final product is a data set of consistent monthly precipitation data with a spatial resolution of 2.5° from 1979 to the present. It is acknowledged that satellite observations are subject to various errors and uncertainties. The error sources arise from uncertainties in retrieval algorithms, data acquisition, data postprocessing, infrequent overpasses, etc. (Hong et al. 2006; AghaKouchak et al. 2009). However, previous studies show that bias-adjusted data sets exhibit reasonable agreement with ground-based observations (Gebremichael et al. 2003; Huffman et al. 2003; Janowiak et al. 2001). The data set used in this study is available to the public through the Global Integrated Drought Monitoring and Prediction System (GIDMaPS; AghaKouchak et al. 2013).

The study area extends from 60°S to 60°N (6,912 pixels) where satellite-based drought data are available. Following (Sheffield and Wood 2008), areas with rainfall below 0.5 mm/day ($<15\text{ mm month}^{-1}$) are masked out of the analysis to avoid unreliable statistics. This procedure eliminates areas in perpetual droughts such as deserts, where a small variability in monthly rainfall alters wet and dry conditions considerably.

3 Method and results

In this paper, and following (Yoon et al. 2012), the 6-month SPI (see McKee et al. 1993) is employed to investigate droughts (see Appendix for details). The drought conditions used in this study are (a) $-2 < \text{SPI} \leq -1$ (moderate to severe droughts) and (b) $\text{SPI} \leq -2$ (extreme droughts). Time series of the areas under drought from January 1980 to January 2012 are derived for moderate to severe droughts ($-2 < \text{SPI} \leq -1$) and extreme droughts ($\text{SPI} \leq -2$) across the global land areas, the Northern Hemisphere (NH), and the Southern Hemisphere (SH). Figures 1 and 2 display areas in moderate to severe drought (Fig. 1) and extreme drought (Fig. 2) over the past three decades. In both figures, the solid black line represents the global land, whereas the dashed red and dotted blue lines show land in the NH and SH, respectively.

For $\text{SPI} \leq -1$, on average 13–15 % of the global land is under drought, whereas 2–3 % is in extreme drought

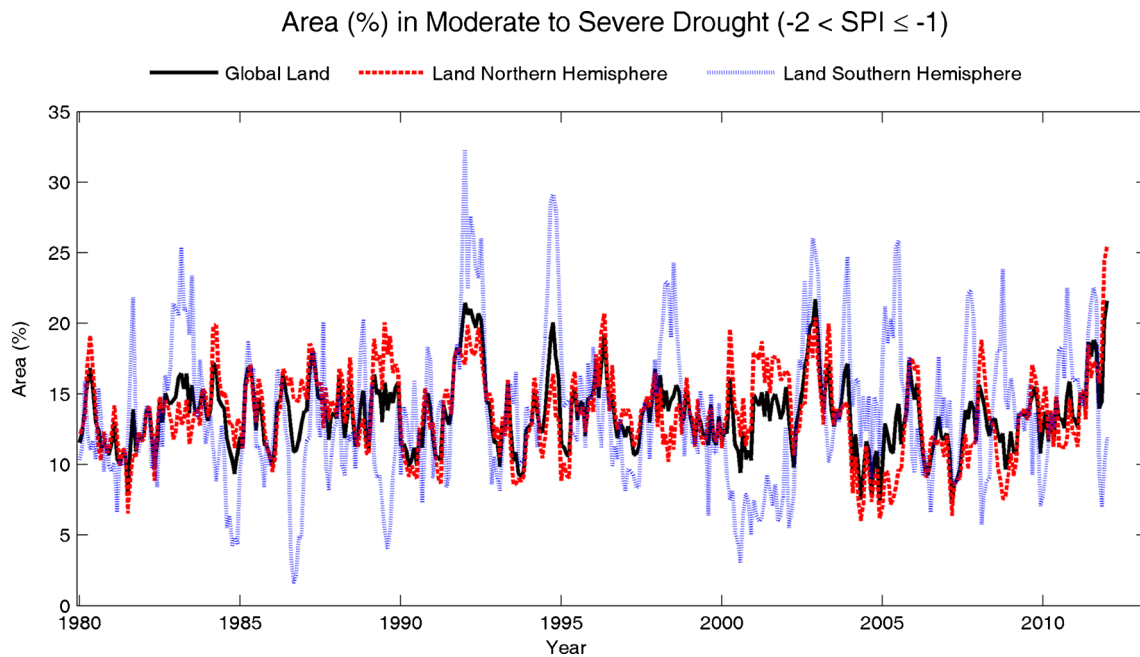


Fig. 1 Area (percent) in moderate to severe drought ($-2 < \text{SPI} \leq -1$) for the global land, land in the NH, and land in the SH from 1980 to 2012

($\text{SPI} \leq -2$) condition ($\text{SPI} \leq -1 = -2 < \text{SPI} \leq -1 + \text{SPI} \leq -2$). Because SPI is a standardized index, for $-2 < \text{SPI} \leq -1$, the areas (percent) under drought for land (13.52 %), land in the NH (13.51 %), and land in the SH (13.53 %) are very similar. It should be noted that SPI normalizes precipitation relative to historical observations using the standard normal distribution (see [Appendix](#)). For

this reason, the area under the SPI graph for a fixed threshold (e.g., $\text{SPI} < -1$) would be quite similar at different locations/regions. While the mean values of area under drought are similar, the results indicate that droughts over land in the SH are far more variable than those over land in the NH (see [Figs. 1 and 2](#)). As shown in [Fig. 1](#), the variability (range of changes) in fraction of land in moderate to severe drought

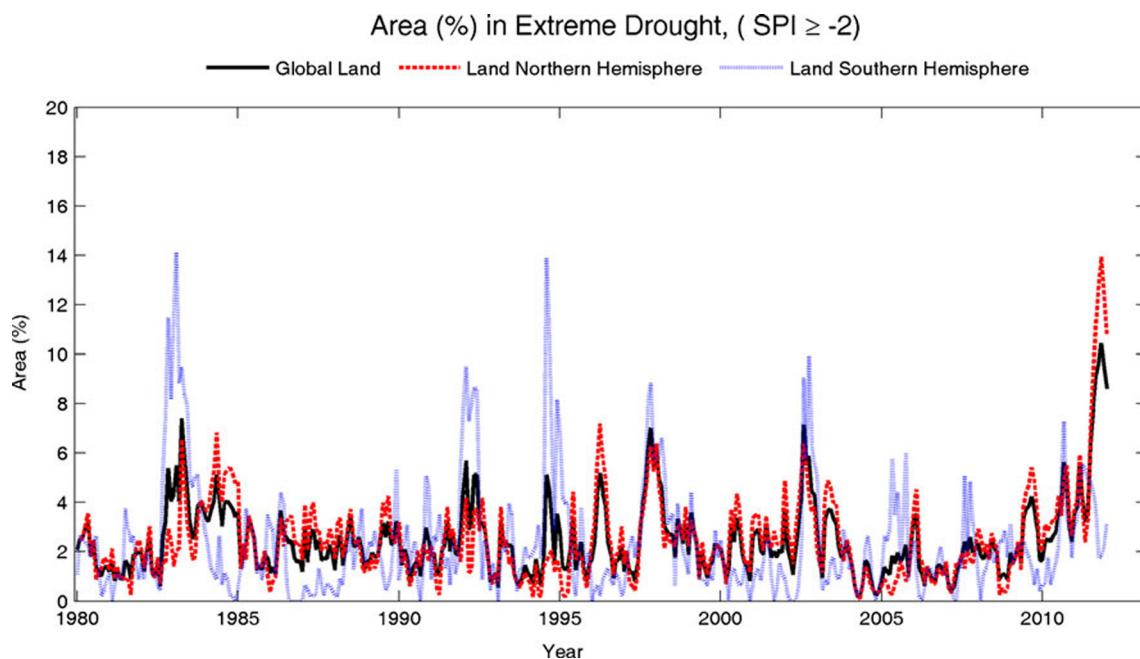


Fig. 2 Area (percent) in extreme drought (6-month $\text{SPI} \leq -2$) for the global land, land in the NH, and land in the SH from 1980 to 2012

conditions ($-2 < \text{SPI} \leq -1$) is approximately 19 % in the NH, while it is over 30 % in the SH.

As demonstrated in Figs. 1 and 2, more peaks of land under drought can be observed in the SH compared to the NH. Table 1 lists the mean and range of areas under drought for the global land, the NH land, and the SH land separately. From Figs. 1 and 2 and Table 1, one can conclude that, in terms of both amplitude and frequency, land droughts are more variable in the SH than in the NH. Table 1 indicates that the mean and ranges of area under extreme droughts are similar for land, the NH land, and the SH land. The higher variability of drought in the SH can be explained with the fact that lands in the SH are less contiguous and more scattered than lands in the NH. Those distinct areas in the SH undergo very diverse climatic regimes, and this could be a reason that drought coverage over land varies in the SH much more than in the NH. Naturally, the larger and more contiguous land exhibits less variability.

The trends of changes in area under drought are investigated using the nonparametric Mann–Kendall test (Mann 1945; Kendall 1976; Fatichi 2009), which compares the relative magnitudes of the samples and provides information on whether the null hypothesis of no trend in the data can be rejected or not (Helsel and Hirsh 2010). The test returns the so-called H value, which is either 0, indicating that the null hypothesis is correct and no trend is detected, or 1, indicating the detection of a trend. For a random variable $X(x_1, x_2, \dots, x_n)$, the Mann–Kendall test can be expressed as (Mann 1945; Kendall 1976):

$$S = \sum_{i=1}^{n-1} \sum_{j=i+1}^n \text{sgn}(x_j - x_i) \quad (1)$$

where n is the sample size and

$$\text{sgn} = \begin{cases} +1 & \text{if}(x_j - x_i) > 0 \\ 0 & \text{if}(x_j - x_i) = 0 \\ -1 & \text{if}(x_j - x_i) < 0 \end{cases} \quad (2)$$

In the Mann–Kendall test, a large positive value of the so-called S statistics in Eq. 1 implies an increasing trend, while a large negative S indicates a decreasing trend.

Table 1 Mean and range of area (percent) in drought

	$-2 < \text{SPI} \leq -1$		$\text{SPI} \leq -2$	
	Range	Mean	Range	Mean
Global land	14.49	13.52	10.25	2.47
Land NH	19.43	13.51	13.84	2.51
Land SH	30.68	13.53	14.13	2.36

NH Northern Hemisphere, SH Southern Hemisphere

Following (Yue et al. 2002), the significance of the trend can be obtained using the z test, where z denotes the standardized z test statistic (Yue et al. 2002), and σ is standard deviation that can be approximated as (Kendall 1976):

$$z = \begin{cases} \frac{S-1}{\sigma(S)} & \text{if } S > 0 \\ 0 & \text{if } S = 0 \\ \frac{S+1}{\sigma(S)} & \text{if } S < 0 \end{cases} \quad (3)$$

where z denotes the standardized z test statistic (Yue et al. 2002), and σ is standard deviation that can be approximated as (Kendall 1976):

$$\sigma(S) = \sqrt{\frac{n(n-1)(2n+5)}{18}} \quad (4)$$

Throughout the study, a significance level of 0.05 is used for analysis, indicating 95 % confidence. Table 2 summarizes the trend analysis results for drought area (percent) over the past three decades. In this table, column 3 shows the H value, where 1 indicates a trend at the significance level of 0.05 and 0 indicates no trend. The P values in column 4 represent the probability of receiving the values of the data under the null hypothesis that there is no trend and, thus, a small P value indicates higher confidence.

As shown in Table 2, a significant trend (H value = 1) has been observed over the lands in the SH. Here, P values below 0.05 are considered as significant trends (confidence of 95 %). A smaller P value implies more confidence in the presence of a trend. The P values of trend analyses over land and land in the NH indicate no trend (significant increase) in the area of land under drought over the past three decades. Our findings are consistent with those of Sheffield et al. (2012) who argued that, based on more realistic observations of drought-related variables, little change has been observed in droughts over the past decades.

Table 2 Trends in the area under drought over the past three decades based on the Mann–Kendall test

		H value	P value
Global land	$\text{SPI} \leq -1$	0	0.799
	$\text{SPI} \leq -2$	0	0.908
Land NH	$\text{SPI} \leq -1$	0	0.156
	$\text{SPI} \leq -2$	0	0.452
Land SH	$\text{SPI} \leq -1$	1	0.04
	$\text{SPI} \leq -2$	0	0.8

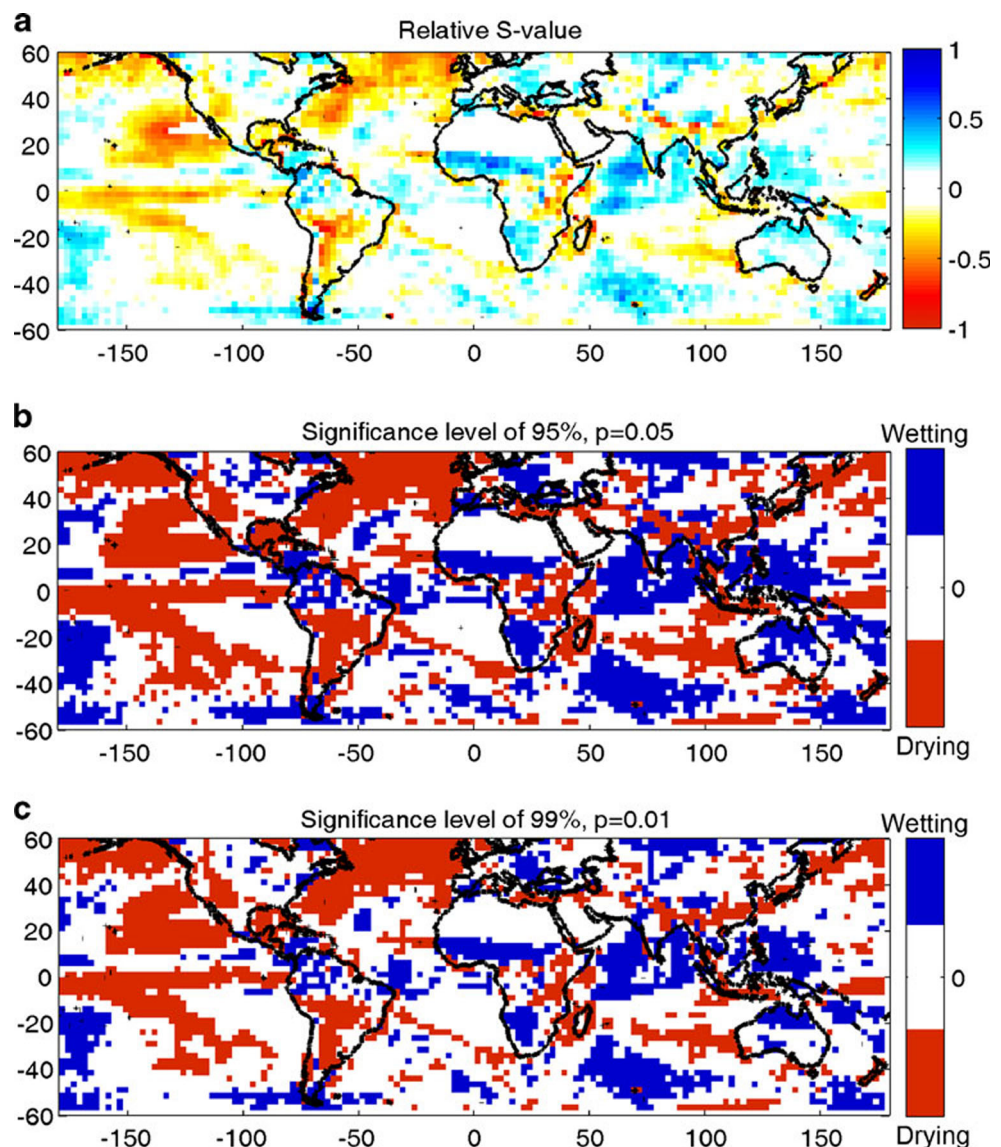
Column 3 shows the H value, where 1 indicates a trend at the significance level of 0.05 and 0 indicates no trend. The P values in column 4 represent the probability of receiving the values of the data under the null hypothesis that there is no trend and, thus, a small P value indicates higher confidence

Based on model simulations, Dai (2011) concluded that global land areas in drought (defined as the bottom 20 % of the local simulated Palmer Drought Severity Index, PDSI) varied between 14 and 16 % from 1950 to 1982, when a sudden increase of approximately 10 % occurred. Thereafter, an upward trend for the spatial extent of areas in drought was demonstrated in Dai (2011). While our results concur with the fraction of areas in drought, we observed a significant increasing trend for land only in the SH in moderate to severe ($-2 < \text{SPI} \leq -1$) drought conditions. No significant trends have been observed for the remaining land areas (e.g., land in the NH)—see column 3 in Table 2. It should be noted that the results presented in this paper cannot be directly compared with those in Dai (2011) because (a) the presented results are based on meteorological drought (SPI), while the results in Dai (2011) are based on the PDSI; (b)

different climatology and data records are used than those used in Dai (2011); (c) different thresholds of droughts are used in the two studies; and (d) the presented results are data-driven and model-independent, while the results in Dai (2011) are based on model simulations.

Finally, the Mann–Kendall test is performed in pixel scale to detect drying and wetting trends in precipitation data over the globe. Figure 3 shows a global map of areas with drying, wetting, and no trend for the past three decades. Figure 3a, b uses the significance level of 0.05, while Fig. 3c shows the positive, negative, and lack of trends at the significance level of 0.01. The upper panel (Fig. 3a) displays the relative S value (Fatichi 2009), which is a normalized measure of the cumulative number of positive and negative changes for the pixels in order to emphasize those areas over the globe where trends are stronger. In Fig. 3a, the S

Fig. 3 Global trends of drying and wetting 6-month SPI over the last 32 years expressed **a** as a relative S value between -1 and 1 , where -1 symbolizes the strongest drying trend (decrease in the SPI over time) and 1 indicates the strongest wetting trends (increase in the SPI over time). The *white areas* represent no trends or are masked out due to perpetual drought (precipitation < 0.5 mm/day); **b** areas showing significant drying (*red*) and wetting (*blue*) trends at a significance level of 0.05; and **c** areas showing significant drying (*red*) and wetting (*blue*) trends at a significance level of 0.01



values are normalized from -1 to 1 based on the cumulative number of changes. The closer the S value to -1 , the stronger is the trend of drying. Conversely, an S value close to 1 represents a stronger trend for wet conditions. For better visualization, Fig. 3 presents the areas with significant drying trends in red and areas with significant wetting trends in blue. Areas with no significant positive or negative trends appear as white, and areas of perpetual droughts are masked out to avoid unreliable statistics according to the above. Note that panels b and c of Fig. 3 show the drying (red areas) and wetting (blue areas) trends at 0.05 and 0.01 significance levels, respectively. This indicates higher confidence in the trends provided in Fig. 3c.

Figure 3 indicates that several areas, such as the southwestern United States, Texas and the Gulf of Mexico region, parts of the Amazon, the Horn of Africa, northern India, and parts of the Mediterranean region, are among areas showing significant drying trends over the past three decades. On the other hand, central Africa, Thailand, Taiwan, Central America, northern Australia, and parts of eastern Europe show a wetting trend during the same time span. The results of this study are consistent with local studies on droughts in the southwestern United States (Cayan et al. 2010) and Amazon (Marengo et al. 2008; Marengo et al. 2011).

4 Conclusions and remarks

Numerous studies argue that the Earth's climate is changing rapidly, especially during the second half of the twentieth century (Trenberth 2001). The acceleration of the hydrologic cycle (Trenberth 1999) indicates that certain regions may become drier, while other areas may become wetter. In fact, an increase or decrease in temperature would alter precipitation patterns and frequency and, thus, intensity and occurrence of droughts. Given the significance of understanding past changes in droughts and their frequency of occurrence in order to predict future droughts, this paper analyzes areas under drought over the past three decades. Unlike most previous global drought studies that have been based on climate model simulations, this study is based on satellite-based, gauge-adjusted precipitation observations.

The analysis demonstrates that droughts are more variable over land in the SH than in the NH (see Fig. 1a, b). The variability (range of change) for the fraction of land in moderate to severe drought conditions ($-2 < \text{SPI} \leq -1$) is approximately 19 % in the NH, while it is over 30 % in the SH. This indicates that, in terms of both amplitude and frequency, land droughts are more variable in the SH than in the NH. The results of the Mann–Kendall test reveal that the area of global land under drought conditions does not show a significant trend over the past three decades (see Table 2).

However, after investigating land in the NH and SH separately, the results exhibit a significant positive trend in the land area under drought in the SH, while no significant trend is observed in land in the NH.

Using the analysis of spatial patterns of wetting and drying trends, maps were created from the pixel-based satellite data. The maps show that several regions, such as the southwestern United States, exhibit significant trends in occurrence of droughts. Other areas, such as the Gulf of Mexico region, Texas, parts of the Amazon, the Horn of Africa, northern India, and parts of the Mediterranean region, also show significant drying trends over the past three decades. The global trend maps indicate that central Africa, parts of southwest Asia (e.g., Thailand, Taiwan), Central America, northern Australia, and parts of eastern Europe show wetting trends. The results of this study are consistent with various previous studies showing an increase in droughts for the areas with drying trends.

In conclusion, one objective of this study was to investigate droughts independent of climate models and based on spatial observations. Overall, the results of this satellite-based study disagree with several model-based studies (e.g., Dai 2012) that indicate droughts have been increasing over land. On the other hand, our findings concur with some of the observation-based studies, such as (Sheffield et al. 2012). The authors emphasize the importance of using independent data sets to cross validate climate model simulations. Given that satellite-based climate data records are emerging, we expect that, in the near future, more research will be devoted to investigating spatial patterns of climate extremes using spaceborne observations.

Appendix

Estimating the Standardized Precipitation Index (SPI) involves describing frequency distribution of precipitation using a gamma probability density function:

$$g(x) = \frac{1}{\beta^\alpha \Gamma(\alpha)} x^{\alpha-1} e^{-\frac{x}{\beta}} \quad (5)$$

where α and β are the shape and scale parameters, respectively. In Eq. 5, x denotes positive precipitation amounts and $\Gamma(\alpha)$ is the gamma function. The parameters α and β can be estimated using the maximum likelihood method as (Edwards 1997):

$$\alpha = \frac{1}{4 \left(\ln(\bar{x}) - \frac{\sum \ln(x)}{n} \right)} \left(1 + \sqrt{1 + \frac{4 \left(\ln(\bar{x}) - \frac{\sum \ln(x)}{n} \right)}{3}} \right) \quad (6)$$

and

$$\beta = \frac{\bar{x}}{\alpha} \quad (7)$$

where n is the number of observations. The estimated parameters will then be used to derive the cumulative probability of observed precipitation values for the given month and time scale (e.g., 6 months) over each pixel:

$$G(x) = \frac{1}{\beta^\alpha \Gamma(\alpha)} \int_0^x x^{\alpha-1} e^{-\frac{x}{\beta}} dx \quad (8)$$

Assuming $t = \frac{x}{\beta}$, Eq. 8 reduces to the so-called incomplete cumulative gamma distribution function (Edwards 1997):

$$G(x) = \frac{1}{\Gamma(\alpha)} \int_0^x t^{\alpha-1} e^{-t} dt \quad (9)$$

The above equation is not valid for $x = 0$ (zero precipitation values). To account for zeros, the complete cumulative probability distribution, $H(x)$, can be written as:

$$H(x) = q + (1 - q)G(x) \quad (10)$$

where q and $1 - q$ denote the probabilities of zero and nonzero precipitations, respectively. The SPI is then derived by transforming the cumulative probability (Eq. 10) to the standard normal distribution with a mean of 0 and variance of 1 (McKee et al. 1993).

Acknowledgments The authors would like to thank the editor and reviewers for their thoughtful comments and suggestions on an earlier draft of this paper. This study is supported by the National Science Foundation (NSF, award no. EAR-1316536) and the United States Bureau of Reclamation (USBR, award no. R11AP81451).

References

- Adler R, Huffman G, Chang A, Ferraro R, Xie P, Janowiak J, Rudolf B, Schneider U, Curtis S, Bolvin D, Gruber A, Susskind J, Arkin P (2003) The version-2 Global Precipitation Climatology Project (GPCP) monthly precipitation analysis (1979). *J Hydrometeorol* 4:1147–1167
- AghaKouchak A, Nakhjiri N (2012) A near real-time satellite-based global drought climate data record. *Environ Res Lett* 7(4):044037. doi:10.1088/1748-9326/7/4/044037
- AghaKouchak A, Nasrollahi N, Habib E (2009) Accounting for uncertainties of the TRMM satellite estimates. *Remote Sens* 1(3):606–619
- AghaKouchak A, Easterling D, Hsu K, Schubert S, Sorooshian S (2012a) Extremes in a changing climate. Springer, Dordrecht
- AghaKouchak A, Mehran A, Norouzi H, Behrangi A (2012b) Systematic and random error components in satellite precipitation data sets. *Geophys Res Lett* 39(9):L09406
- AghaKouchak A, Hao Z, Nakhjiri N (2013) The global drought monitoring and prediction system. Tech rep, University of California, Irvine, version 1. <http://drought.eng.uci.edu/>. Accessed 25 Sept 2013
- Alexander L, Zhang X, Peterson T, Caesar J, Gleason B, Klein Tank A, Haylock M, Collins D, Trewin B, Rahimzadeh F, Tagipour A, Ambenje P, Rupa Kumar K, Revadekar J, Griffiths G (2006) Global observed changes in daily climate extremes of temperature. *J Geophys Res* 111:D05109
- Anderson MC, Hain C, Wardlaw B, Pimstein A, Mecikalski JR, Kustas WP (2011) Evaluation of drought indices based on thermal remote sensing of evapotranspiration over the continental United States. *J Clim* 24(8):2025–2044
- Andreadis K, Clark E, Wood A, Hamlet A, Lettenmaier D (2005) Twentieth-century drought in the conterminous United States. *J Hydrometeorol* 6(6):985–1001
- Cayan DR, Das T, Pierce DW, Barnett TP, Tyree M, Gershunov A (2010) Future dryness in the southwest US and the hydrology of the early 21st century drought. *Proc Natl Acad Sci USA* 107(50):21271–21276
- Coelho CAS, Goddard L (2009) El Niño-induced tropical droughts in climate change projections. *J Clim* 22(23):6456–6476
- Dai A (2011) Drought under global warming: a review. *Wiley Interdiscip Rev Clim Chang* 2(1):45–65
- Dai A (2012) Increasing drought under global warming in observations and models. *Nat Clim Chang* 2:52–58. doi:10.1038/nclimate1633
- Dirmeyer P, Gao X, Gao Z, Oki T, Hanasaki M (2006) The Global Soil Wetness Project (GSWP-2). *Bull Am Meteorol Soc* 87:1381–1397
- Easterling D (2012) Global data sets for analysis of climate extremes. In: AghaKouchak A, Easterling D, Hsu K, Schubert S, Sorooshian S (eds) Extremes in a changing climate: detection, analysis and uncertainty. Springer, New York. doi: 10.1007/978-94-007-4479-012
- Edwards D (1997) Characteristics of 20th century drought in the United States at multiple time scales. Tech rep, Colorado State University, Fort Collins, Colorado
- Fatichi S (2009) Mann-Kendall test. Tech rep, Dipartimento Ingegneria Civile e Ambientale, Università degli Studi di Firenze
- Frich P, Alexander L, Della-Marta P, Gleason B, Haylock M, Klein Tank A, Peterson T (2002) Observed coherent changes in climatic extremes during the second half of the twentieth century. *Clim Res* 19:193–212
- Gebremichael M, Krajewski WF, Morrissey M, Langerud D, Huffman GJ, Adler R (2003) Error uncertainty analysis of GPCP monthly rainfall products: a data-based simulation study. *J Appl Meteorol* 42(12):1837–1848
- Hao Z, AghaKouchak A (2013a) Multivariate standardized drought index: a parametric multi-index model. *Adv Water Resour* 57:12–18. doi:10.1016/j.advwatres.2013.03.009
- Hao Z, AghaKouchak APT (2013b) Changes in concurrent monthly precipitation and temperature extremes. *Environ Res Lett*. doi:10.1088/1748-9326/8/3/034014
- Hayes M, Svoboda M, Wilhite D, Vanyarkho O (1999) Monitoring the 1996 drought using the Standardized Precipitation Index. *Bull Am Meteorol Soc* 80:429–438
- Helsel D, Hirsh R (2010) Trend analysis. Tech rep. In: Helsel DR, Hirsh RM (eds) Statistical methods in water resources. U.S. Geological Survey, Reston
- Hong Y, Hsu K, Moradkhani H, Sorooshian S (2006) Uncertainty quantification of satellite precipitation estimation and Monte Carlo assessment of the error propagation into hydrologic response. *Water Resour Res* 42(8):w08421
- Hsu K, Gao X, Sorooshian S, Gupta H (1997) Precipitation estimation from remotely sensed information using artificial neural networks. *J Appl Meteorol* 36:1176–1190
- Huffman G, Adler R, Bolvin D, Nelkin E (2003) Estimating uncertainty in GPCP and TRMM multi-satellite precipitation estimates. In: IUGG XXIII: state of the planet: frontiers and challenges, Sapporo, Japan, International Union of Geodesy and Geophysics, CD-ROM, JSM18
- Huffman G, Adler R, Bolvin D, Gu G, Nelkin E, Bowman K, Stocker E, Wolff D (2007) The TRMM multi-satellite precipitation

- analysis: quasi-global, multiyear, combined-sensor precipitation estimates at fine scale. *J Hydrometeorol* 8:38–55
- Janowiak J, Gruber A, Curtis S, Huffman G, Adler R, Xie P (2001) Evaluation and comparison of the CMAP and GPCP oceanic precipitation analyses. WCRP. In: SCOR workshop on intercomparison and validation of ocean-atmosphere flux fields, Bolger Center, Potomac, MD (Washington, DC area)
- Kendall M (1976) Rank correlation methods, 4th edn. Griffin, London
- Kirono DGC, Kent DM (2011) Assessment of rainfall and potential evaporation from global climate models and its implications for Australian regional drought projection. *Int J Climatol* 31(9):1295–1308
- Mann H (1945) Nonparametric tests against trend. *Econometrica* 13:245–259
- Marengo JA, Nobre CA, Tomasella J, Oyama MD, De Oliveira GS, De Oliveira R, Camargo H, Alves LM, Brown IF (2008) The drought of Amazonia in 2005. *J Clim* 21(3):495–516
- Marengo JA, Tomasella J, Alves LM, Soares WR, Rodriguez DA (2011) The drought of 2010 in the context of historical droughts in the Amazon region. *Geophys Res Lett* 38:L12703
- McKee T, Doesken N, Kleist J (1993) The relationship of drought frequency and duration to time scales. Proceedings of the 8th conference of applied climatology, 17–22 Jan 1993. American Meteorological Society, Anaheim, pp 179–184
- Mehran A, AghaKouchak A (2013) Capabilities of satellite precipitation datasets to estimate heavy precipitation rates at different temporal accumulations. *Hydrol Process*. doi:[10.1002/hyp.9779](https://doi.org/10.1002/hyp.9779)
- Mo K (2008) Model based drought indices over the United States. *J Hydrometeorol* 9:1212–1230
- Robock A, Luo L, Wood E, Wen F, Mitchell K, Houser P, Schaake J, Lohmann D, Cosgrove B, Sheffield J, Duan Q, Higgins R, Pinker R, Tarpley J, Basara J, Crawford K (2004) Evaluation of the north American land data assimilation system over the southern Great Plains during the warm season. *J Geophys Res*:109
- Serinaldi F, Bonaccorso B., Cancelliere A., Grimaldi S. (2009) Probabilistic characterization of drought properties through copulas. *Phys Chem Earth* 34(10–12):596–605
- Sheffield J, Wood EF (2008) Projected changes in drought occurrence under future global warming from multi-model, multi-scenario, IPCC AR4 simulations. *Clim Dyn* 31(1):79–105
- Sheffield J, Goteti G, Wen F, Wood E (2004) A simulated soil moisture based drought analysis for the United States. *J Geophys Res Atmos* 109(D24)
- Sheffield J, Wood E, Roderick M (2012) Little change in global drought over the past 60 years. *Nat* 491(7424):435–438
- Shiau J (2006) Fitting drought duration and severity with two-dimensional copulas. *Water Resour Manag* 20(5):795–815
- Shukla S., Wood A. (2008) Use of a standardized runoff index for characterizing hydrologic drought. *Geophys Res Lett* 35(2):102405
- Sorooshian S, Hsu K, Gao X, Gupta H, Imam B, Braithwaite D (2000) Evolution of the PERSIANN system satellite-based estimates of tropical rainfall. *Bull Am Meteorol Soc* 81(9):2035–2046
- Sorooshian S, AghaKouchak A, Arkin P, Eylander J, Foufoula-Georgiou E, Harmon R, Hendrickx JMH, Imam B, Kuligowski R, Skahill B, Skofronick-Jackson G (2011) Advanced concepts on remote sensing of precipitation at multiple scales. *Bull Am Meteorol Soc* 92(10):1353–1357
- Tian Y, Peters-Lidard C, Eylander J, Joyce R, Huffman G, Adler R, Hsu K, Turk F, Garcia M, Zeng J (2009) Component analysis of errors in satellite-based precipitation estimates. *J Geophys Res* 114:D24101
- Trenberth K (1999) Conceptual framework for changes of extremes of the hydrological cycle with climate change. *Clim Chang* 42(1):327–339
- Trenberth K (2001) Climate variability and global warming. *Sci* 293(5527):48–49
- Turk FJ, Arkin P, Ebert EE, Sapiano MRP (2008) Evaluating high-resolution precipitation products. *Bull Am Meteorol Soc* 89(12):1911–1916
- Wang D, Hejazi M, Cai X, Valocchi AJ (2011) Climate change impact on meteorological, agricultural, and hydrological drought in central Illinois. *Water Resour Res* 47:W09527
- Wardlow B, Anderson M, Verdin J (2012) Remote sensing of drought. CRC, Boca Raton
- WCRP (2010) A WCRP white paper on drought predictability and prediction in a changing climate: assessing current predictive knowledge and capabilities, user requirements and research priorities. Tech rep, World Climate Research Programme
- Wehner M (2012) Methods of projecting future changes in extremes. In: AghaKouchak A, Easterling D, Hsu K, Schubert S, Sorooshian S (eds) *Extremes in a changing climate: detection, analysis and uncertainty*. Springer, New York. doi: [10.1007/978-94-007-4479-08](https://doi.org/10.1007/978-94-007-4479-08)
- Wilhite D, Glantz M (1985) Understanding the drought phenomenon: the role of definitions. *Water Int* 10:111–120
- WMO (2009) Inter-regional workshop on indices and early warning systems for drought. Lincoln, Nebraska, USA, 8–11 December 2009, World Meteorological Organization
- Yoon J-H, Mo K, Wood EF (2012) Dynamic-model-based seasonal prediction of meteorological drought over the contiguous United States. *J Hydrometeorol* 13(2):463–482
- Yue S, Pilon P, Cavadias G (2002) Power of the Mann–Kendall and Spearman's rho tests for detecting monotonic trends in hydrological series. *J Hydrol* 259(1):254–271